Optical, structural, mechanical and thermal characterization of antioxidant ethylene vinyl alcohol copolymer films containing betalain-rich beetroot

Cejudo-Bastante, María Jesús, Cejudo-Bastante, Cristina, Cran, Marlene, Heredia, Francisco J and Bigger, Stephen W (2020) Optical, structural, mechanical and thermal characterization of antioxidant ethylene vinyl alcohol copolymer films containing betalain-rich beetroot. Food Packaging and Shelf Life, 24. ISSN 2214-2894

Optical, structural, mechanical and thermal characterization of antioxidant ethylene vinyl alcohol copolymer films containing betalain-rich beetroot

María Jesús Cejudo-Bastante[a]*, Cristina Cejudo-Bastante[b], Marlene J. Cran[c], Francisco J. Heredia[a], Stephen W. Bigger[c]

[a] Food Colour and Quality Lab., Área de Nutrición y Bromatología, Facultad de Farmacia, Universidad de Sevilla, 41012 Sevilla, Spain

[b] Chemical Engineering and Food Technology Department, Wine and Agrifood Research Institute (IVAGRO), Universidad de Cádiz, 11510, Spain

[c] Institute for Sustainable Industries and Liveable Cities, Victoria University, Werribee Campus, PO Box 14428, Melbourne 8001, Australia

María Jesús Cejudo-Bastante: mjcejudo@us.es

Cristina Cejudo-Bastante: cristina.cejudo@uca.es

Marlene J. Cran: Marlene.Cran@vu.edu.au

Francisco J. Heredia: heredia@us.es

Stephen W. Bigger: Stephen.Bigger@vu.edu.au

**** Corresponding author:***

María Jesús Cejudo-Bastante
Food Colour & Quality Lab., Área de Nutrición y Bromatología, Facultad de Farmacia, Universidad de Sevilla, 41012, Sevilla, Spain
Tel.: +34 954556760
e-mail: mjcejudo@us.es

Abstract

New antioxidant films based on ethylene vinyl alcohol (EVOH) copolymer containing betalain-rich red beet were successfully manufactured and characterized to develop bioactive packaging for food products. Two types of red beet (powder and extract) at different proportions (0.1, 0.5, 1.0, 1.5, 2.0 and 2.5% (w/w)) were incorporated into EVOH films, with attention focused on the optical, chemical, thermal, structural, and mechanical and antioxidant properties. The incorporation of any red beet type into EVOH resulted in purple-colored and semi-crystalline thin films, without modifying their thermal stability and mechanical properties. The addition of the beet extract led to a film with higher color intensity, antioxidant activity and lower water loss rate, whereas the addition of powdered beet resulted in an improved UV barrier compared to the extract. The results showed that new antioxidant food packaging films based on EVOH could be realized by utilizing beetroot extract or powder obtained from natural resources.

Keywords: Red beet; ethylene vinyl alcohol copolymer; film properties; antioxidant packaging; betalains.

1. Introduction

In recent years, demand for minimally-processed, preservative-free foods with longer shelf-lives and oxidation prevention has increased significantly. In this regard, the food industry is focusing on the modification of food packaging as one possible solution to meet this need. The development of new packaging films using bioactive substances obtained from natural resources, which are typically related to the enhancement of food safety and quality, is currently growing (Tawakkal, Cran, & Bigger, 2014). However, it must be taken into consideration that the addition of bioactive compounds to the packaging must not compromise the integrity of the film and therefore its optimal physical, mechanical and thermal properties must be maintained.

Red beet (*Beta vulgaris* L. sp) belongs to the *Chenopodiaceae* family and is a red taproot rich in polyphenols and water-soluble pigments called betalains. These pigments (classified as red-violet betacyanins and yellow-orange betaxanthins) are claimed to have beneficial properties for human health such as antioxidant activity, antiviral, anti-inflammatory and anticarcinogenic effects (Moreno, García-Viguera, Gil, & Gil-Izquierdo, 2008; Strack, Vogt, & Schliemann, 2003; Vinson, Hao, Su, & Zubik, 1998). Moreover, betanin, the major betalain present in *Beta vulgaris*, is also a natural colorant approved by the United States and the European Union as a food additive (E-162), and has been related to the inhibition of lipid peroxidation and tumor cell proliferation (Reddy, Alexander-Lindo, & Nair, 2005).

A broad range of polymeric materials and different types of bioactive compounds have been studied in order to develop new food packaging materials. For example, Cejudo Bastante, Casas Cardoso, Mantell Serrano, and Martínez de la Ossa (2017) recently developed a novel antioxidant food packaging film using supercritical impregnation of multilayer PET/PP films with olive leaf extract by-product. The resulting film was deemed to be suitable as an active food packaging material with acceptable thermal, structural and mechanical properties depending on the impregnation conditions. Other bioactive compounds used in active packaging include green tea extract and oregano essential oil, which were added to ethylene-vinyl alcohol copolymer (EVOH) (V. Muriel-Galet, Cerisuelo, López-Carballo, Aucejo, Gavara, & Hernández-Muñoz, 2013; V. Muriel-Galet, Cran, Bigger, Hernández-Muñoz, & Gavara, 2015). However, although the extracts provided antioxidant activity, the crystallinity of the EVOH film was affected. A minor impact on water permeability and thermal stability, and an enhancement of tensile properties of EVOH films was observed after the addition of cinnamaldehyde in the film-formulation compared to the control film with no additives (Ma, Li, & Wang, 2017).

Recent studies have reported the use of betalain-rich raw materials as additives for various biopolymers and edible films have been reported in order to develop active film systems (Aparicio-Fernández, Vega-Ahuatzin, Ochoa-Velasco, Cid-Pérez, Hernández-Carranza, & Ávila-Sosa, 2018; Gutiérrez, Suniaga, Monsalve, & García, 2016; Iahnke, Costa, De Oliveira Rios, & Flôres, 2016; Lozano-Navarro, Díaz-Zavala, Velasco-Santos, Martínez-Hernández, Tijerina-Ramos, García-Hernández, et al., 2017; Tran, Athanassiou, Basit, & Bayer, 2017). However, there are limited studies reporting the incorporation of red beet as bioactive ingredient and source of betalains into packaging. In one example, a recent study reported the use of red beetroot powder as an antioxidant agent in a packaging film formulation (Tran, Athanassiou, Basit, & Bayer, 2017), achieving an improvement of Young's modulus of starch-based bioelastomers. In another example, biocomposite films were manufactured by embedding different concentrations of beetroot residue powder into films based on residues of gelatin capsules (Iahnke, Costa, De Oliveira Rios, & Flôres, 2016), resulting in a promising antioxidant material with good thermal properties.

However, to the best of our knowledge, there are no reports of the incorporation of beetroot powders in EVOH films for food packaging.

The present study was therefore aimed to develop a film based on EVOH combined with betalain-rich beetroot using a casting procedure. Two different preparations of red beet (powder and extract) and a diverse range of concentrations were formulated. Detailed experimental work is presented in order to characterize the physical-mechanical and structural properties as well as the thermal and antioxidant properties of the resulting films.

2. Material and Methods

2.1. Chemicals and Reagents

Ethylene vinyl alcohol copolymer with a 29% molar content of ethylene (EVOH29 Soarnol DT2904RB®) was supplied by the Nippon Synthetic Chemical Company (Osaka, Japan). Chemical reagents 1-propanol, absolute ethanol, 2,2-diphenyl-1-picrylhydrazyl (95% free radical) were purchased from Rowe Scientific (Australia). Sodium ascorbate was purchased from Panreac (Barcelona, Spain) and methanol (AR grade) from J. T. Baker (Baker, Mallinckrodt, Mexico). Water (HPLC grade) was obtained using a Milli-Q plus water purification system (Millipore Corp., Bedford, MA, USA). Methanol (HPLC grade) and formic acid (HPLC grade) were obtained from Fischer Chemical (UK) and Sigma-Aldrich (St. Louis, MO, USA), respectively.

2.2. Red Beet Samples

Red beetroots (*Beta Vulgaris* L., sp. Var. Pablo) were collected in the south-west area of Andalucía (Sevilla, Spain). Samples of mature fruits according to visual characteristics and similar size were collected up to a weight of *ca.* 2 kg. The beets were peeled and cut into small pieces (1 cm^2) prior to lyophilization (Labconco, MO, USA) to obtain the red beet powder (RBP), which was stored in darkness until analysis and subsequent use. To obtain the red beet extract (RBE) of the betalains from RBP, 3 mL of methanol and 3 mL of water containing 50 mM sodium ascorbate was added to 0.1 g of lyophilized RBP. After stirring at 200 rpm for 10 min in darkness, samples were centrifuged at 4000 rpm at 10ºC for 5 min, according to the method proposed by Cejudo-Bastante, Chaalal, Louaileche, Parrado, and Heredia (2014). The supernatant was separated, and the process was repeated with the same extraction solution. Finally, the procedure was repeated with 100% methanol until the complete discoloration of the plant tissue was achieved. The RBE was then lyophilized. All extraction processes were performed in triplicate.

2.3. Evaluation of Red Beet Composition

An Agilent 1200 chromatographic system equipped with a quaternary pump, a UV-visible diode-array detector, an automatic injector, and ChemStation software (Palo Alto, USA) was used for separation, identification, and semi-quantification of the main betalains of the RBP. Prior to direct injection, all the samples were filtered through a 0.45 μm Nylon filter (E0034, Análisis Vínicos, Spain). Analyses were performed using a Zorbax C18 column (250 × 4.6 mm, 5 μm particle size), a flow rate of 1 mL min^{-1} at 25°C, an injection volume of 20 µL, with eluents comprised of 1% (v/v) formic acid in water (eA) and methanol (eB). The separation of betalains was performed using the following elution profile: 100% eA, 0 min; 90% eA, 10% eB, 20 min; 70% eA, 30% eB, 30 min; 100% eB, 35 min; then 100% eA, 40 min, with the purpose of re-establishing the initial conditions (Cejudo-Bastante, Chaalal, Louaileche, Parrado, & Heredia, 2014). The resulting UV-visible spectra of the separated extracts were recorded from 200 to 800 nm with a bandwidth of 1.0 nm and the betacyanins and betaxanthins were monitored at 535 and 482 nm, respectively. The identification of each chromatographic peak was tentatively assigned by its visible spectral characteristics in comparison with its retention times and their visible spectral characteristics according to the method proposed by Cejudo-Bastante, Chaalal, Louaileche, Parrado, and Heredia (2014).

2.4. Film Preparation

The film samples were prepared in duplicate according to the method proposed by Virginia Muriel-Galet, Cerisuelo, López-Carballo, Lara, Gavara, and Hernández-Muñoz (2012) with some modifications. Pellets of EVOH (1 g) were dissolved in 10 mL of a 1-propanol/water mixture at a ratio of 1:1 (v/v) at 70°C. When the solution had cooled below 30°C, the betalain samples (RBP and RBE) were added at different proportions of 0.1, 0.5, 1.0, 1.5, 2.0 and 2.5% (w/w) with respect to the mass of EVOH in the solution. The casting coater (Porometer Memcast™, Belgium) was located in a laboratory fume hood with air extraction. The films were prepared, under dark conditions, by spreading the solution with a coating bar on a warm flat stainless steel surface (35°C) that facilitated the evaporation of the solvent and minimized degradation of the betalain compounds (Herbach, Stintzing, & Carle, 2006). Films devoid of RBP or RBE were prepared as controls and all film samples were stored under dry and dark conditions in aluminum foil until testing. All films were manageable and had a homogeneous average thickness of 3-4 µm (n = 5) measured using a digital micrometer (Schut IP54, The Netherlands) with 0.001 mm precision.

2.5. Structural Analysis

Changes in the chemical composition of the films after the RBP and RBE addition with respect to the EVOH control film were evaluated using Fourier-transform infrared (FTIR) spectroscopic analysis. A Perkin Elmer Frontier™ FTIR spectrophotometer (Waltham, USA) fitted with a diamond crystal attenuated total reflectance (ATR) accessory was used to record the spectra of the samples. An average of 16 scans at a resolution of 4 cm^{-1} over the frequency range 4000–650 cm^{-1} was obtained for each sample with measurements performed at 25°C and in triplicate.

2.6. Optical Properties

The color of the film was measured using a Konica Minolta CR-400 Chroma Meter (Konica Minolta Sensing, Inc., Osaka, Japan). The films were placed on a white standard tile surface and three measurements were taken from different parts of the film. The parameters of lightness (L^*, where 0 = black through to 100 = white), the hue angle (h_{ab}, which is the qualitative color attribute defined as red (0°/360°), yellow (90°), green (180°) or blue (270°)), and color saturation (C^*_{ab}) were determined for each film sample.

The absorption of the films was determined using UV–visible spectroscopy. A piece of film was cut and directly placed in a quartz cell (10 mm path length glass cell) with air as a reference (Kuorwel, Cran, Sonneveld, Miltz, & Bigger, 2014). The transmittance of each sample was scanned over the wavelength range of 200–800 nm using a Varian CARY 300 Scan UV-visible spectrophotometer. The transparency (T) was calculated by measuring the percent transmittance of light at a wavelength of 600 nm (%T_{600}) (T=-log %T_{600}/b) and the opacity (O) was calculated using the average absorbance at 500 nm (A_{500}) (O=A_{500}xb), taking into account the film thickness in mm (b) for all the measurements (Lozano-Navarro, et al., 2017). All measurements were performed in triplicate.

2.7. Antioxidant Activity

The antioxidant activity of the films was determined using the 2,2-diphenyl-1-picrylhydrazyl (DPPH) free radical assay (Brand-Williams, Cuvelier, & Berset, 1995). Pieces of film measuring *ca.* 2 cm^2 were introduced to 4 mL of 6 $\times 10^{-5}$ mol L^{-1} DPPH in ethanol, according to the method described by (Cejudo Bastante, Casas Cardoso, Mantell Serrano, & Martínez de la Ossa, 2017). The decrease in the UV absorbance was monitored using a Varian CARY 300 Scan UV-visible spectrophotometer at 517 nm in darkness until a steady state had been achieved (60 min). The percentage of inhibition (%I) measured as the quantity of DPPH that reacts with a given amount of antioxidant, was calculated by measuring the initial DPPH absorbance (A_0) and final absorbance at 1 h (A_i) where $\%I = 100 \times (A_0 - A_i)/A_0$. Analyses were carried out in duplicate and the results were expressed as %I/100 mg of film.

2.8. Thermal Analysis

The thermal phase transitions were determined by differential scanning calorimetry (DSC) using a Mettler-Toledo Differential Scanning Calorimetry DSC1 instrument. Samples of *ca.* 5 mg were encapsulated in aluminum pans, using an empty aluminum pan (40 µL) as a reference. Thermograms were obtained by heating samples from 35°C to 220°C, with heating and cooling rates of 10°C min^{-1}. The samples were maintained under a 50 mL min^{-1} nitrogen gas flow during the analysis and single experiments were performed (Wrona, Cran, Nerín, & Bigger, 2017). The melting temperature (T_m) and the melting enthalpy (ΔH_m) were calculated using STAR^e Evaluation Software (Mettler-Toledo, version 11.00) for data acquisition and analysis. The percentage of crystallinity (%X_c) was calculated using $\%X_c = 100 \times \Delta H_m / \Delta H^{\circ}_m$, where ΔH°_m is the melting enthalpy of 100% pure crystalline EVOH (157.8 J g^{-1}) (Cerrada, Pérez, Pereña, & Benavente, 1998).

Thermogravimetric (TG) analyses were performed using a Mettler-Toledo TGA/DSC1 instrument. Samples of 4 to 5 mg of film were cut into small pieces and heated from 20 to 600°C at 10°C min^{-1} under a nitrogen atmosphere flow rate of 50 mL min^{-1} in order to prevent any thermo-oxidative degradation. The data collected with the STAR^e Evaluation software were further analyzed to determine the reaction model of thermal decomposition and the apparent activation energy, E_a, using the algorithms described by Bigger, Cran, and Tawakkal (2015).

2.9. Imaging and Morphology

Scanning electron microscopy (SEM) was utilized to investigate the morphology of the films after the addition of RBP and RBE. Micrographs of the surface of the films with the highest percentages of these additives were obtained using a Hitachi TM3030 Plus Tabletop SEM. Samples were mounted on an aluminum sample holder and were coated with iridium for 30 s using a sputter coater (Cressington, UK) prior to obtaining the images at magnifications of 5×, 200× and 500× under high vacuum and an accelerating voltage of 10 kV.

2.10. Water Vapor Transmission Rate

The water vapor transmission rate (WVTR) of the EVOH films and those containing RBP or RBE was determined in accordance with ASTM E96-93 with some modifications. Glass vials of 10 mL capacity were filled with 5 mL of water and 1.3 cm diameter pieces of film were placed over the vials to form a seal. The glass vials were then stored at room temperature in a desiccator containing silica or at 35°C in an air-circulating oven (< 50% of relative humidity, respectively). The vials were weighed daily for up to 20 days using an analytical balance to measure the WVTR which was determined using WVTR=($\Delta m/\Delta tA$), where $\Delta m/\Delta t$ is the mass of water lost per time (g/day) and A is the exposed surface area of the film (m^2) (Shahriari, Mohseni, & Yahyaei, 2019).

2.11. Mechanical Properties

The mechanical characteristics of the films were measured with a Model 4301 Instron Universal Testing Machine with a load cell of 5 kN in accordance with ASTM D882. For each set of samples, five tensile specimens with dimensions of 14 cm × 2 cm were prepared. Each tensile test was conducted using a cross-head speed of 10 mm min^{-1}. The

Young's modulus (YM), tensile stress at maximum load (or ultimate tensile strength, UTS) and the elongation at break (EAB) were calculated from the stress-strain curves and the data obtained using Instron BlueHill Series IX software.

2.12. Statistical Analysis

Statistica v.8.0 software (Statistica, 2007) was used for performing all statistical analyses. Univariate analyses of variance (Tukey test and ANOVA) ($p < 0.05$) were applied to establish whether the mean values of the sample data differed significantly in each case.

3. Results and Discussion

3.1. Red Beet Composition

Fig. 1 shows the chromatogram and the identification of the betalain profile (betacyanins and betaxanthins) of the RBP used in this work. Among the betacyanins, betanin and isobetanin are well-known compounds present in red beetroots (Montes-Lora, Rodríguez-Pulido, Cejudo-Bastante, & Heredia, 2018). With regard to betaxanthins, vulgaxanthin I (glutamine-betaxanthin) and other betaxanthins derived from histidine, aminobutyric acid, proline, valine, isoleucine, leucine and phenylalanine, were also identified. Some of these are rarely reported in this raw material. Betanin was clearly the major betalain present in all the RBP samples, followed by isobetanin and vulgaxanthin I, representing around 95% of the total betalains and this is consistent with other reported works (Montes-Lora, Rodríguez-Pulido, Cejudo-Bastante, & Heredia, 2018).

3.2. Structural Analysis of Films

The FTIR spectra of the control EVOH films and those containing RBP or RBE were measured and normalized to an unchanging peak. The peak at 850 cm^{-1} due to -CH rocking vibrations of the EVOH was selected as one appearing in all spectra that was not expected to change with different levels of RBP or RBE (Topolniak, Gardette, & Therias, 2015). The incorporation of either RBP or RBE into the EVOH film showed similar trends with regard to the entire FTIR spectra, thus, only the spectra of EVOH control film, EVOH film containing 2.5% (w/w) RBE and pure RBE are presented in Fig. 2. In comparison with the spectrum of the control EVOH film, the intensity of the peaks at 3330, 2929 and 2853 cm^{-1} increased when RBE was added to the film. These peaks correspond to hydroxyl vibrations, NH_2 stretching, symmetric and asymmetric CH_2 and CH stretching vibrations, respectively (Abdollahi, Taghizadeh, & Savani, 2018; Zhang, Li, Huang, Ren, & Huang, 2018). This may be due to the presence of the polar betalains in the RBE which contain several -OH and -NH bonds and aromatic groups (Montes-Lora, Rodríguez-Pulido, Cejudo-Bastante, & Heredia, 2018; Saroufim, Celauro, & Mistretta, 2018). The carbonyl vibrations of the -NH amide groups at 1658 cm^{-1} also increase with the presence of RBE which is clearly observed as a broad peak in the pure RBE spectrum (Peter, Kenyo, Renner, Krohnke, & Pukanszky, 2014). Interactions of EVOH with RBE are suggested with the presence of strong -CO stretching vibrations arising from the -COH bonds at 1092 cm^{-1} due to the presence of alcohols in the film-forming solution (Abdollahi, Taghizadeh, & Savani, 2018). When higher quantities of RBE were added, a bathochromic shift was observed with the peak slightly shifting from 1092 to 1086 cm^{-1}. Moreover, a general broadening of this peak in the presence of RBE is observed which may be evidence of hydrogen bonding between RBE and EVOH (Arunbabu, Sannigrahi, & Jana, 2010).

3.3. Film Optical Properties

Table 1 shows the color parameters of the EVOH control film and those containing RBE and RBP at different proportions. Optical properties are of utmost importance since they reflect the colour and UV barrier properties of the film. Regarding CIELAB parameters (L^*, a^*, b^*, C^*_{ab}, h_{ab}), the control EVOH films were almost colorless (a^*=-0.41; b^*=3.21), whereas the films containing beetroot showed a significantly (p < 0.05) more purplish tonality (h_{ab}) and a reduced lightness (L^*) compared to the control EVOH films as expected. These changes were significant ($p < 0.05$) when concentrations from 1.5% of RBE or RBP were embedded to the film. In the case of EVOH/RBE, a significantly ($p < 0.05$) greater color intensity (C^*_{ab}) was also observed in comparison to the control films. The reduction of lightness and changes in C^*_{ab} and h_{ab} parameters as a consequence of the incorporation of natural extracts and beetroot powder into the EVOH copolymer and other materials have also been observed by other researchers (V. Muriel-Galet, Cran, Bigger, Hernández-Muñoz, & Gavara, 2015; Wrona, Cran, Nerín, & Bigger, 2017; Zamudio-Flores, Ochoa-Reyes, Ornelas-Paz, Tirado-Gallegos, Bello-Pérez, Rubio-Ríos, et al., 2015).

Considering transparency and opacity, the incorporation of RBP or RBE provided a more opaque and less transparent film. This was found to be significant ($p < 0.05$) even with the lowest addition of 0.1% (w/w) of the RBE or RBP (Table 1) and increased substantially when the proportion of RBE or RBP increased. Similar results were reported by Lozano-Navarro, et al. (2017) in chitosan–starch films with different natural extracts. The resulting films had UV-visible light barrier properties that can potentially minimize the accelerated decomposition of some photosensitive food (Iahnke, Costa, De Oliveira Rios, & Flôres, 2016; Ma, Li, & Wang, 2017).

A comparison between the two types of beet additive showed that EVOH/RBP films presented statistically ($p < 0.05$) lower chromatic intensity and tonality compared to EVOH/RBE. This could be due to the other residual plant materials present in the RBP samples (Gaikwad, Lee, & Lee, 2016; Iahnke, Costa, De Oliveira Rios, & Flôres, 2016) and, indeed, the lower content of betalains at the same proportion of RB.

3.4. Antioxidant Activity

Fig. 3 shows the antioxidant activity of control films and those containing different quantities of RBE and RBP expressed as the %I of the DPPH radical. The results show that the control EVOH films imparted little or no antioxidant activity but the addition of 1% (w/w) and greater of RBP or RBE showed some antioxidant effect (%I around 10%). The %I of EVOH/RBE films was significantly ($p < 0.05$) higher than that of EVOH/RBP films at all concentrations of additives (between 12-25%), suggesting that RBP also contains a considerable number of compounds that are not antioxidants. As such, although both types of films offered antioxidant properties, higher amounts of RBP are needed to offer the same antioxidant capacity as RBE. Although very few studies have reported active films based on EVOH and beetroot, considerable antioxidant activities have also been described in other films due to the presence of betalain-rich materials and/or other copolymers. Examples include starch-based bio-elastomers functionalized with red beetroot (Tran, Athanassiou, Basit, & Bayer, 2017), carboxymethyl cellulose edible films with *Opuntia-ficus indica* peel (Aparicio-Fernández, Vega-Ahuatzin, Ochoa-Velasco, Cid-Pérez, Hernández-Carranza, & Ávila-Sosa, 2018), and films based on gelatin capsules and beetroot residues (Iahnke, Costa, De Oliveira Rios, & Flôres, 2016).

3.5. Film Thermal Properties

Table 2 shows the various thermal parameters obtained from DSC thermograms of EVOH, EVOH/RBP and EVOH/RBE films containing different levels of the additives. The T_m value of the control film was *ca.* 19ºC lower than the manufacturer's value for extruded EVOH films and this may be attributed to the casting fabrication process that, in turn, influences the polymer crystallization (Muriel-Galet, Cran, Bigger, Hernández-Muñoz, & Gavara, 2015). The incorporation of either RBP or RBE into the EVOH film did not significantly ($p < 0.05$) affect the T_m values when compared to the pure EVOH film. The values of ΔH_m and $\%X_c$, however, were significantly ($p < 0.05$) increased with the addition of 0.5-1% (w/w) of each additive. This is particularly evident in the case of increasing RBP for both parameters and in the case of RBE for $\%X_c$. The higher energy required to melt the crystalline structures suggests that some structural modifications have taken place that affect the crystallization process (Franco-Urquiza, Santana, Gámez-Pérez, Martínez, & Maspoch, 2010). This result is in accordance with the results obtained in the FTIR analysis whereby the increase in hydrogen bonding resulting from the presence of betalains that contain a large number of OH groups could limit the chain mobility, favor the intermolecular and intramolecular forces, and thereby increase the cohesive energy (Lagaron, Catalá, & Gavara, 2004). This trend was more noticeable when higher levels of RBP or RBE were added and EVOH/RBP films were generally less rigid and easier to break than EVOH/RBE films indicating a more irregular crystalline structure (Muriel-Galet, Cran, Bigger, Hernández-Muñoz, & Gavara, 2015). The latter may be due to the interruptions to crystallization that are caused by the presence of other non-betalainic compounds (i.e. residual plant materials), or by the lower betalain content in RBP compared to RBE at the same proportion.

The TG curves for EVOH and EVOH/RBE 2.5% (Fig. 4(a)) show that the main decomposition step is slightly lower for the sample containing RBE. There is also a small step in the TG curve that occurs between 80 and 100 °C which represents the evaporation of the residual solvent (1-propanol/water). This evaporation at this early heating stage may have influenced the crystallinity observed in the DSC measurements (Khan, Ryan, Blau, & Coleman, 2007). The decomposition of the RB at the lower temperature may have also influenced the measured crystallinity for the samples containing RBP or RBE. The first derivative curves of the TG thermograms (see Fig. 4(b)) revealed that the thermal degradation of the films occurred mainly over a single step, confirmed by a large peak at around 350-400 °C (Ma, Li, & Wang, 2017). Moreover, there is no separate step that can be attributed to the presence of either RBP or RBE in the TG profile of the EVOH/RBP sample.

Table 3 shows the values of onset and endset temperatures obtained for the thermal degradation of all films. A discernible mass loss of 75-80% occurred between 363 and 395ºC in the case of the EVOH control films corresponding to the degradation of the polymer. The incorporation or either RBP or RBE into the film did not result in any significant ($p < 0.05$) changes in onset and endset temperatures, with the exception of EVOH films containing higher quantities of RBE of 2-2.5% (w/w) (Fig. 4). In these cases, the onset and endset temperatures were lower than that of the EVOH control film (Table 3), which is in contrast to the results observed by Ma, Li, and Wang (2017) when cinnamaldehyde was incorporated into EVOH films. In the present study, the addition of RBP and low quantities of RBE did not influence the thermal stability of the films, however, 2% (w/w) and greater of RBE slightly lowered the onset of thermal decomposition of the film. Similar thermal trends have also been described by Iahnke, Costa, De Oliveira Rios, and Flôres (2016) when red beet powder was incorporated into a gelatin-based film.

Table 3 also shows the values of the apparent activation energy, E_a, for the degradation process of the control film and films containing RBP and RBE at different proportions. The E_a of the main degradation step was extracted by performing kinetic analyses on the TG data in accordance with the method described by Bigger, Cran, and Tawakkal (2015). The method consists of an iterative computerized technique that obtains the best fitting model under the same test conditions by using several and well-established models applied to the mass loss curve. In general, all films were strongly fitted to the contracting volume (R3) model ($R^2 > 0.97$) and the incorporation of either RBP or RBE into the

EVOH film did not significantly alter the E_a of any film regardless of the type and proportion of the additive (Table 3). These findings would reinforce the importance of these films within the food packaging field. Moreover, the high thermal stability of these materials would allow their use under typical sterilization procedures, required for food-based applications.

3.6. Film Surface Morphology

The SEM micrographs at different magnification of the EVOH films and those incorporated with the highest content of RBE and RBP are presented in Fig. 5. It is evident that the surfaces of the EVOH and EVOH/RBE films are both particularly homogeneous, with a smooth, continuous and well-connected network (Fig. 5a and 5b, respectively). In contrast, some particles were observed on the surface of the EVOH/RBP films reflecting a heterogeneous texture and the presence of agglomerates (Fig. 5c) which may be due to the presence of insoluble residual plant materials and fibers in the RBP (Iahnke, Costa, De Oliveira Rios, & Flôres, 2016). This is further shown in the SEM micrograph of the pure RBP which revealed irregular inclusions and rough surfaces of the various components (Fig. 5d).

3.7. Film Water Barrier Properties

Fig. 6 shows the WVTR of the EVOH control film and those containing RBP and RBE at different compositions at 25°C and 35°C where the WVTR value of each sample was the average of all the measurements recorded over the twenty days of the experiment. In general, the WVTR was typically lower than 1% per day which might be expected for EVOH film which is known for its barrier properties. However, some significant ($p < 0.05$) differences between films were observed at the higher temperature of 35ºC whereby levels 1.5% (w/w) and higher of RBP significantly ($p < 0.05$) increased the WVTR compared to films tested at 20ºC. This finding is consistent with that reported by Rojas-

Graü, Avena-Bustillos, Olsen, Friedman, Henika, Martín-Belloso, et al. (2007) who incorporated 0.1% (w/w) of carvacrol into alginate–apple puree films and found an increased WVTR at higher temperatures. The present results are also consistent with those of Kuorwel, Cran, Sonneveld, Miltz, and Bigger (2014) and Pruneda, Peralta-Hernández, Esquivel, Lee, Godínez, and Mendoza (2008), who added natural agents and Mexican oregano into starch-based and soy protein isolate films, respectively. The slight increase of WVTR may be due to high levels of insoluble plant materials in RBP which are not completely dispersed in the film-forming solution. In addition, the large agglomerates from the RBP could create voids at the EVOH interface that inhibit the development of a continuous layer during film casting, thereby resulting in a more porous structure which could weaken the resultant films (Tran, Athanassiou, Basit, & Bayer, 2017).

3.8. Mechanical Properties

The mechanical properties of films are important to achieve their potential use as food packaging, thus the YM, UTS and EAB parameters were measured. Only EVOH control films and those containing the highest levels of RBP or RBE were taken into account since the YM, UTS and EAB of the films remained relatively unchanged when RBE and RBP were added as shown in Table S1. This may be due to the presence of soluble compounds which do not interrupt the EVOH matrix despite the hydrogen bond interactions (Aparicio-Fernández, Vega-Ahuatzin, Ochoa-Velasco, Cid-Pérez, Hernández-Carranza, & Ávila-Sosa, 2018). These results are similar to those obtained by Iahnke, Costa, De Oliveira Rios, and Flôres (2016) who studied the tensile strength of films based on gelatin and beetroot residues and studies of extruded EVOH films have also reported similar UTS values of 30-40 MPa (Peter, Kenyo, Renner, Krohnke, & Pukanszky, 2014). It would be expected that films obtained by casting, such as those in the present study, would have mechanical properties that are different to those obtained by extrusion or other processes. However, casting is recommended in the case of incorporating heat sensitive compounds such as betalains in order to prevent thermal decomposition which can occur at relatively low temperatures (Herbach, Stintzing, & Carle, 2006; Selig, Celli, Tan, La, Mills, Webley, et al., 2018).

4. Conclusions

Films based on EVOH containing red beet powder and extracts at different proportions were successfully manufactured by a casting procedure. The red beet was found to adequately disperse in the copolymer in both the powder and extract forms, without detriment to the thermal stability or mechanical properties. The resulting films were also slightly more crystalline, had significant antioxidant properties, and the modification to the color of the films may potentially contribute to a higher resistance to UV light. The water barrier properties were slightly reduced, particularly in the case of the powder form of the additive, which could potentially be minimized by using these films in multilayer formulations or coatings. Although the powdered form of the red beet contained some insoluble components, there were no significant benefits obtained by incorporating the extract form of the red beet when compared to the powdered form. The results show some promise for food packaging applications where antioxidant activity is required with the added benefit of barrier and UV properties.

Acknowledgments

This work was supported by the Ministerio de Educación, Cultura y Deporte by the concession of a José Castillejo grant. Authors thank the Biology Service of Centro de Investigación Tecnología e Innovación (CITIUS), Universidad de Sevilla, for technical assistance.

Declaration of interest. None.

References

Abdollahi, R., Taghizadeh, M. T., & Savani, S. (2018). Thermal and mechanical properties of graphene oxide nanocomposite hydrogel based on poly (acrylic acid) grafted onto amylose. *Polymer Degradation and Stability, 147*, 151-158.

Aparicio-Fernández, X., Vega-Ahuatzin, A., Ochoa-Velasco, C. E., Cid-Pérez, S., Hernández-Carranza, P., & Ávila-Sosa, R. (2018). Physical and Antioxidant Characterization of Edible Films Added with Red Prickly Pear (Opuntia ficus-indica L.) cv. San Martín Peel and/or Its Aqueous Extracts. *Food and Bioprocess Technology, 11*(2), 368-379.

Arunbabu, D., Sannigrahi, A., & Jana, T. (2010). Blends of Polybenzimidazole and Poly(vinylidene fluoride) for Use in a Fuel Cell. *Journal of Physical Chemistry B*, *112*, 5305-5310.

Bigger, S. W., Cran, M. J., & Tawakkal, I. S. M. A. (2015). Two novel algorithms for the thermogravimetric assessment of polymer degradation under non-isothermal conditions. *Polymer Testing, 43*, 139-146.

Brand-Williams, W., Cuvelier, M. E., & Berset, C. (1995). Use of a free radical method to evaluate antioxidant activity. *LWT - Food Science and Technology*, *28*(1), 25-30.

Cejudo-Bastante, M. J., Chaalal, M., Louaileche, H., Parrado, J., & Heredia, F. J. (2014). Betalain profile, phenolic content, and color characterization of different parts and varieties of opuntia ficus-indica. *Journal of Agricultural and Food Chemistry, 62*(33), 8491-8499.

Cejudo Bastante, C., Casas Cardoso, L., Mantell Serrano, C., & Martínez de la Ossa, E. J. (2017). Supercritical impregnation of food packaging films to provide antioxidant properties. *Journal of Supercritical Fluids*, *128*, 200-207.

Cerrada, M. L., Pérez, E., Pereña, J. M., & Benavente, R. (1998). Wide-angle X-ray diffraction study of the phase behavior of vinyl alcohol-ethylene copolymers. *Macromolecules, 31*(8), 2559-2564.

Franco-Urquiza, E., Santana, O. O., Gámez-Pérez, J., Martínez, A. B., & Maspoch, M. L. (2010). Influence of processing on the ethylene-vinyl alcohol (EVOH) properties: Application of the successive self-nucleation and annealing (SSA) technique. *Express Polymer Letters, 4*(3), 153-160.

Gaikwad, K. K., Lee, J. Y., & Lee, Y. S. (2016). Development of polyvinyl alcohol and apple pomace bio-composite film with antioxidant properties for active food packaging application. *Journal of Food Science and Technology, 53*(3), 1608-1619.

Gutiérrez, T. J., Suniaga, J., Monsalve, A., & García, N. L. (2016). Influence of beet flour on the relationship surface-properties of edible and intelligent films made from native and modified plantain flour. *Food Hydrocolloids, 54*, 234-244.

Herbach, K. M., Stintzing, F. C., & Carle, R. (2006). Betalain stability and degradation - Structural and chromatic aspects. *Journal of Food Science*, *71*(4), R41-R50.

Iahnke, A. O. E. S., Costa, T. M. H., De Oliveira Rios, A., & Flôres, S. H. (2016). Antioxidant films based on gelatin capsules and minimally processed beet root (Beta vulgaris L. var. Conditiva) residues. *Journal of Applied Polymer Science, 133*(10).

Khan, U., Ryan, K., Blau, W. J., & Coleman, J. N. (2007). The effect of solvent choice on the mechanical properties of carbon nanotube-polymer composites. *Composites Science and Technology*, *67*(15-16), 3158-3167.

Kuorwel, K. K., Cran, M. J., Sonneveld, K., Miltz, J., & Bigger, S. W. (2014). Physico-mechanical properties of starch-based films containing naturally derived antimicrobial agents. *Packaging Technology and Science*, *27*(2), 149-159.

Lagaron, J. M., Catalá, R., & Gavara, R. (2004). Structural characteristics defining high barrier properties in polymeric materials. *Materials Science and Technology*, *20*(1), 1-7.

Lozano-Navarro, J. I., Díaz-Zavala, N. P., Velasco-Santos, C., Martínez-Hernández, A. L., Tijerina-Ramos, B. I., García-Hernández, M., Rivera-Armenta, J. L., Páramo-García, U., & Reyes-de la Torre, A. I. (2017). Antimicrobial, optical and mechanical properties of Chitosan–Starch films with natural extracts. *International Journal of Molecular Sciences*, *18*(5).

Ma, Y., Li, L., & Wang, Y. (2017). Development of antimicrobial active film containing CINnamaldehyde and its application to snakehead (Ophiocephalus argus) fish. *Journal of Food Process Engineering*, *40*(5).

Montes-Lora, S., Rodríguez-Pulido, F. J., Cejudo-Bastante, M. J., & Heredia, F. J. (2018). Implications of the Red Beet Ripening on the Colour and Betalain Composition Relationships. *Plant Foods for Human Nutrition*, *73*(3), 216-221.

Moreno, D. A., García-Viguera, C., Gil, J. I., & Gil-Izquierdo, A. (2008). Betalains in the era of global agri-food science, technology and nutritional health. *Phytochemistry Reviews, 7*(2), 261-280.

Muriel-Galet, V., Cerisuelo, J. P., López-Carballo, G., Aucejo, S., Gavara, R., & Hernández-Muñoz, P. (2013). Evaluation of EVOH-coated PP films with oregano essential oil and citral to improve the shelf-life of packaged salad. *Food Control*, *30*(1), 137-143.

Muriel-Galet, V., Cerisuelo, J. P., López-Carballo, G., Lara, M., Gavara, R., & Hernández-Muñoz, P. (2012). Development of antimicrobial films for microbiological control of packaged salad. *International Journal of Food Microbiology, 157*(2), 195-201.

Muriel-Galet, V., Cran, M. J., Bigger, S. W., Hernández-Muñoz, P., & Gavara, R. (2015). Antioxidant and antimicrobial properties of ethylene vinyl alcohol copolymer films based on the release of oregano essential oil and green tea extract components. *Journal of Food Engineering, 149*, 9-16.

Peter, Z., Kenyo, C., Renner, K., Krohnke, C., & Pukanszky, B. (2014). Decreased oxygen permeability of EVOH through molecular interactions. *Express Polymer Letters, 8*(10), 756-766.

Pruneda, E., Peralta-Hernández, J. M., Esquivel, K., Lee, S. Y., Godínez, L. A., & Mendoza, S. (2008). Water vapor permeability, mechanical properties and antioxidant effect of Mexican oregano-soy based edible films. *Journal of Food Science, 73*(6), C488-C493.

Reddy, M. K., Alexander-Lindo, R. L., & Nair, M. G. (2005). Relative inhibition of lipid peroxidation, cyclooxygenase enzymes, and human tumor cell proliferation by natural food colors. *Journal of Agricultural and Food Chemistry, 53*(23), 9268-9273.

Rojas-Graü, M. A., Avena-Bustillos, R. J., Olsen, C., Friedman, M., Henika, P. R., Martín-Belloso, O., Pan, Z., & McHugh, T. H. (2007). Effects of plant essential oils and oil compounds on mechanical, barrier and antimicrobial properties of alginate-apple puree edible films. *Journal of Food Engineering, 81*(3), 634-641.

Saroufim, E., Celauro, C., & Mistretta, M. C. (2018). A simple interpretation of the effect of the polymer type on the properties of PMBs for road paving applications. *Construction and Building Materials*, *158*, 114-123.

Selig, M. J., Celli, G. B., Tan, C., La, E., Mills, E., Webley, A.-D., Padilla-Zakour, O. I., & Abbaspourrad, A. (2018). High pressure processing of beet extract complexed with anionic polysaccharides enhances red color thermal stability at low pH. *Food Hydrocolloids*, *80*, 292-297.

Statistica. (2007). StatSoft Inc. STATISTICA (data analysis software system). In 8 ed.). Tulsa, OK.

Strack, D., Vogt, T., & Schliemann, W. (2003). Recent advances in betalain research. *Phytochemistry*, *62*(3), 247-269.

Tawakkal, I. S. M. A., Cran, M. J., & Bigger, S. W. (2014). Effect of kenaf fibre loading and thymol concentration on the mechanical and thermal properties of PLA/kenaf/thymol composites. *Industrial Crops and Products, 61*, 74-83.

Topolniak, I., Gardette, J.-L., & Therias, S. (2015). Influence of zeolite nanoparticles on photostability of ethylene vinyl alcohol copolymer (EVOH). *Polymer Degradation and Stability, 121*, 137-148.

Tran, T. N., Athanassiou, A., Basit, A., & Bayer, I. S. (2017). Starch-based bio-elastomers functionalized with red beetroot natural antioxidant. *Food Chemistry, 216*, 324-333.

Vinson, J. A., Hao, Y., Su, X., & Zubik, L. (1998). Phenol Antioxidant Quantity and Quality in Foods: Vegetables. *Journal of Agricultural and Food Chemistry, 46*(9), 3630-3634.

Wrona, M., Cran, M. J., Nerín, C., & Bigger, S. W. (2017). Development and characterisation of HPMC films containing PLA nanoparticles loaded with green tea extract for food packaging applications. *Carbohydrate Polymers, 156*, 108-117.

Zamudio-Flores, P. B., Ochoa-Reyes, E., Ornelas-Paz, J. D. J., Tirado-Gallegos, J. M., Bello-Pérez, L. A., Rubio-Ríos, A., & Cárdenas-Felix, R. G. (2015). Physicochemical, mechanical, and structural features of oxidized oat and banana starch films enriched with betalains. *Agrociencia, 49*(5), 483-498.

Zhang, S., Li, R., Huang, D., Ren, X., & Huang, T. S. (2018). Antibacterial modification of PET with quaternary ammonium salt and silver particles via electron-beam irradiation. *Materials Science and Engineering C, 85*, 123-129.

FIGURES

Fig. 1. Chromatogram of betalains of RBE at 485 nm: betacyanins: betanin (5) and isobetanin (6); betaxanthins derived from: histidine (muscaarin, 1), glutamine (vulgaxanthin I, 2), aminobutyric acid (3), proline (indicaxanthin, 4), valine (7), isoleucine (8), leucine (vulgaxanthin IV, 9), and phenylalanine (10).

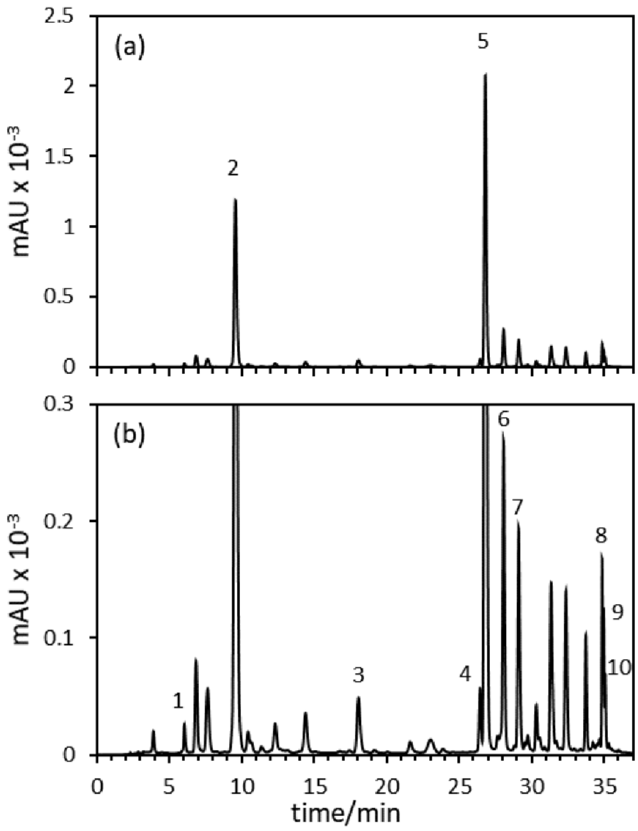

Fig. 2. FTIR-ATR spectra of EVOH control film, EVOH film containing 2.5% RBE, and pure RBE.

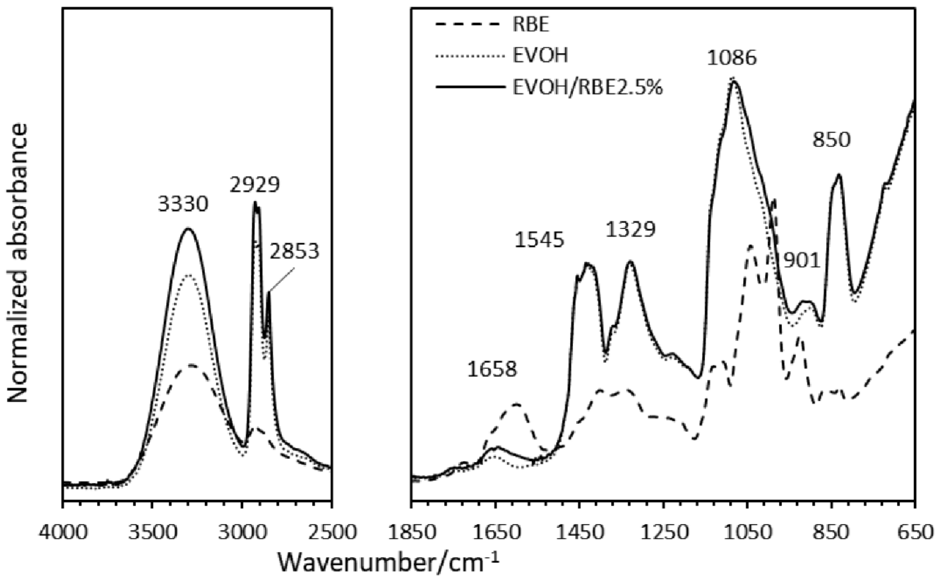

Fig. 3. Percentage of AOX inhibition of EVOH control film and those containing different proportions of RBP and RBE.

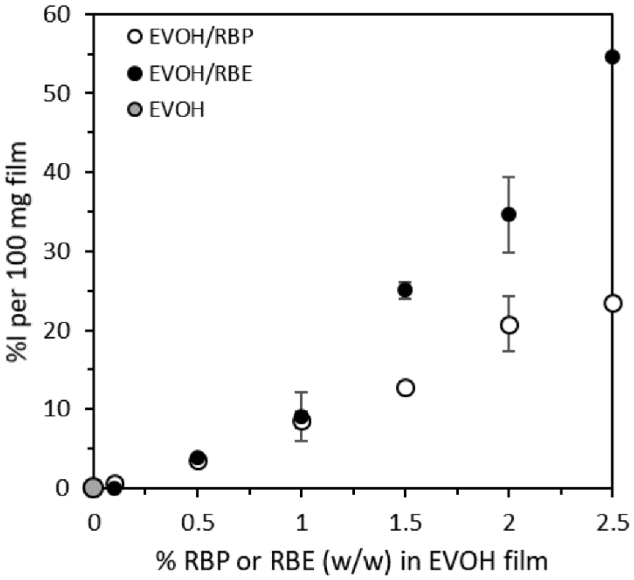

Fig. 4. TG thermograms of EVOH and EVOH film containing 2.5% (w/w) RBE: (a) normalized mass-loss curves and (b) first derivative of mass-loss curves.

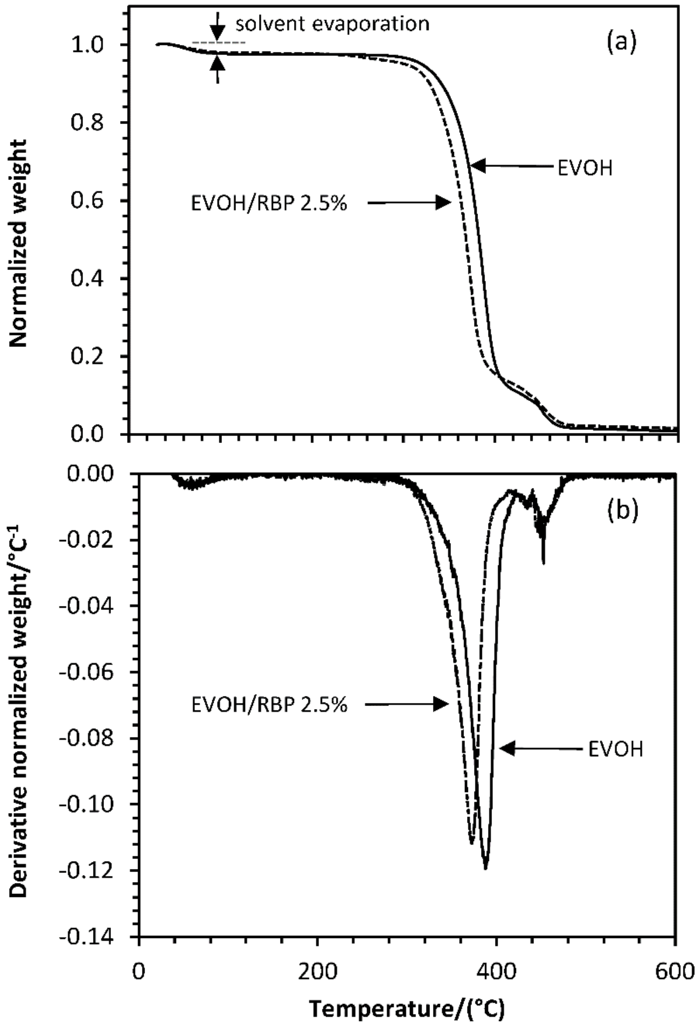

Fig. 5. SEM images of the surfaces of: (a) EVOH film; (b) EVOH film containing 2.5% (w/w) RBE; (c) EVOH film containing 2.5% (w/w) RBP; and (d) pure RBP.

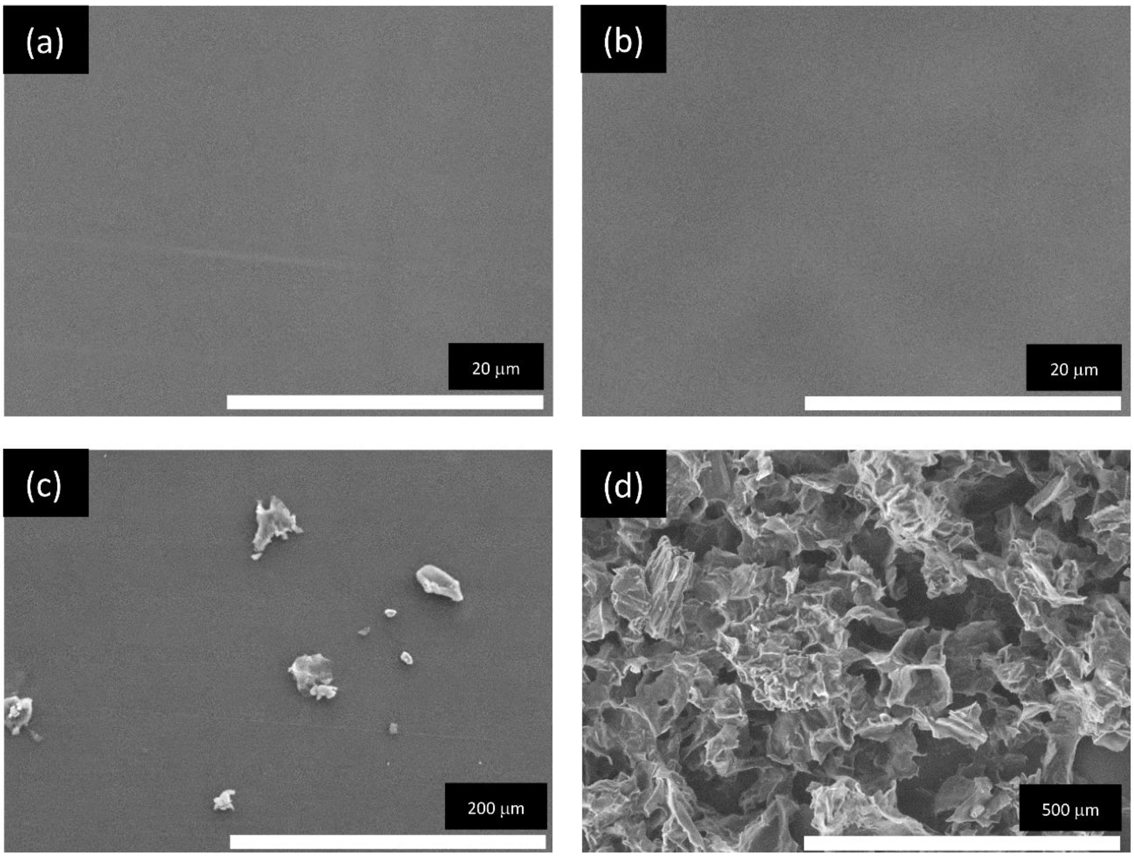

Fig. 6. Water vapor transmission rate (WVTR) through EVOH films containing different proportions of RBP and RBE.

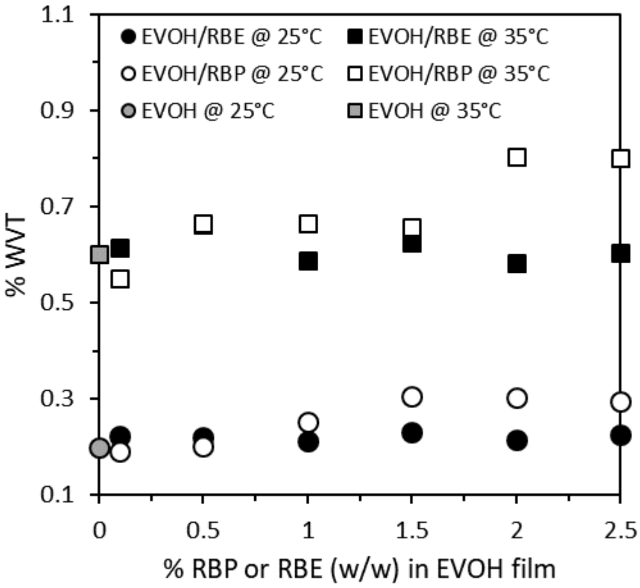

Table 1. Colorimetric characteristics of pure EVOH film and EVOH films containing different proportions of RBP and RBE

	% RB	L^*		C^*_{ab}		h_{ab}		Transparency		Opacity	
EVOH	0.0	95.75 ± 0.09	bA	3.25 ± 0.04	aA	97.24 ± 1.06	aB	1165.8 ± 11.9	aA	0.15 ± 0.01	aA
EVOH/RBP	0.1	95.83 ± 0.09	AB	3.32 ± 0.10	A	98.27 ± 0.07	B	643.67 ± 7.07	BC	0.25 ± 0.01	BC
	0.5	95.44 ± 0.29	B	3.42 ± 0.08	AB	93.40 ± 0.41	B	644.00 ± 3.30	BC	0.25 ± 0.01	BC
	1.0	95.09 ± 0.43	B	3.25 ± 0.01	A	83.89 ± 8.33	B	531.41 ± 2.51	DEFG	0.32 ± 0.01	DEFG
	1.5	94.98 ± 0.17	B	3.13 ± 0.05	A	79.53 ± 3.95	A	544.17 ± 9.05	DEF	0.30 ± 0.01	DEFG
	2.0	95.39 ± 0.11	B	3.20 ± 0.03	A	83.77 ± 1.75	B	549.43 ± 1.21	DEF	0.29 ± 0.00	DEFG
	2.5	94.85 ± 0.25	A	3.16 ± 0.12	A	80.81 ± 5.25	A	517.89 ± 1.58	G	0.29 ± 0.01	DEFG
EVOH/RBE	0.1	95.53 ± 0.25	b	3.29 ± 0.00	a	98.18 ± 1.14	a	961.00 ± 2.83	b	0.17 ± 0.00	b
	0.5	95.42 ± 0.01	b	3.44 ± 0.00	b	95.46 ± 1.35	ab	720.19 ± 1.86	c	0.22 ± 0.00	c
	1.0	95.21 ± 0.13	b	3.53 ± 0.14	b	90.07 ± 2.42	bc	637.17 ± 3.54	def	0.24 ± 0.01	def
	1.5	95.12 ± 0.07	b	3.64 ± 0.05	bc	87.81 ± 1.44	c	630.83 ± 1.18	def	0.23 ± 0.00	cdef
	2.0	95.02 ± 0.20	a	3.71 ± 0.10	bc	84.40 ± 2.20	c	623.48 ± 3.23	def	0.25 ± 0.01	def
	2.5	94.63 ± 0.21	a	3.98 ± 0.10	c	76.67 ± 2.14	d	580.93 ± 9.58	g	0.29 ± 0.00	g

Different upper-case and lower-case letters in the same column denote significant differences according to Tukey test ($p < 0.05$) between EVOH and EVOH/RBP, and EVOH/RBE, respectively.

Table 2. Thermal parameters measured by DSC of pure EVOH film and EVOH films containing different proportions of RBP and RBE.

	% RB	T_m/°C	Endotherm melting widths/°C	ΔH_m/J g^{-1}		%X_c	
EVOH	0.0	169.31 ± 8.07	155.50 - 176.18	57.39 ± 11.99	aA	41.90 ± 0.24	aA
EVOH/RBP	0.1	172.61 ± 12.2	153.98 - 180.05	62.92 ± 2.13	A	39.87 ± 1.35	A
	0.5	180.22 ± 7.35		88.59 ± 7.42	A	56.14 ± 4.70	A
			169.26 - 188.16				B
	1.0	176.92 ± 4.90		76.75 ± 6.96	A	49.86 ± 2.68	A
			160.29 - 183.98				B
	1.5	174.85 ± 4.74	159.29 - 181.40	94.53 ± 14.8	B	59.90 ± 9.37	B
	2.0	175.78 ± 3.77	160.97 - 182.61	94.33 ± 4.74	B	59.78 ± 3.01	B
	2.5	172.01 ± 0.86	153.20 - 178.16	93.22 ± 6.65	B	59.07 ± 4.21	B
EVOH/RBE	0.1	173.37 ± 1.77	156.00 - 180.66	92.87 ± 6.26	b	58.85 ± 3.97	a
	0.5	180.10 ± 0.29	172.18 - 184.63	93.47 ± 3.06	B	59.23 ± 1.94	a
	1.0	174.12 ± 2.16	155.78 - 181.36	96.68 ± 0.84	B	61.26 ± 0.53	b
	1.5	168.64 ± 9.18	146.72 - 175.95	109.22 ± 14.6	b	69.21 ± 9.22	b
	2.0	161.96 ± 5.61	143.64 - 172.40	95.36 ± 3.97	b	60.43 ± 2.51	b
	2.5	174.83 ± 1.34	160.09 - 180.31	102.8 ± 10.0	b	65.11 ± 6.34	b

Different upper-case and lower-case letters in the same column denote significant differences according to Tukey test ($p < 0.05$) between EVOH and EVOH/RBP, and EVOH/RBE, respectively.

Table 3. Onset and endset temperatures and apparent activation energy, E_a, obtained using TG analysis of pure EVOH films and EVOH films containing different proportions of RBP and RBE.

	%RB	Onset T^a^/°C		Endset T^a^/°C		E_a/kJ mol^{-1}	
EVOH	0.0	363.07 ± 0.03	b	395.10 ± 0.18	b	175.00 ± 8.49	bA
EVOH/RBP	0.1	368.50 ± 1.99		404.92 ± 4.53		187.00 ± 4.24	
	0.5	364.81 ± 0.65		395.86 ± 1.99		184.00 ± 15.6	
	1.0	367.62 ± 0.93		397.74 ± 3.12		197.00 ± 9.90	
	1.5	371.06 ± 1.21		391.61 ± 0.40		204.00 ± 20.0	
	2.0	363.93 ± 6.05		391.32 ± 7.67		204.50 ± 12.0	B
	2.5	365.99 ± 0.87		395.75 ± 5.55		191.00 ± 18.4	
EVOH/RBE	0.1	368.28 ± 1.60	b	405.79 ± 0.81	b	186.50 ± 7.78	
	0.5	364.85 ± 1.05	b	401.15 ± 0.51	b	160.50 ± 13.4	
	1.0	362.18 ± 4.44	b	399.73 ± 4.92	b	156.50 ± 9.19	
	1.5	344.18 ± 18.8	b	384.56 ± 13.1	b	155.50 ± 17.7	
	2.0	347.63 ± 0.26	a	384.08 ± 0.52	a	164.00 ± 1.41	
	2.5	346.93 ± 0.37	a	387.70 ± 2.59	a	151.50 ± 7.78	a

Different upper-case and lower-case letters in the same column denote significant differences according to Tukey test ($p < 0.05$) between EVOH and EVOH/RBP, and EVOH/RBE, respectively.

Table S1. Mechanical properties of pure EVOH film and EVOH films containing 2.5% (w/w) RBP and RBE.

	YM/GPa	**UTS/MPa**	**EAB/%**
EVOH	1.50 ± 0.16	28.5 ± 1.5	20.9 ± 1.5
EVOH/RBP	1.13 ± 0.21	24.7 ± 1.4	24.0 ± 1.6
EVOH/RBE	1.34 ± 0.19	24.9 ± 6.9	16.2 ± 1.9